AN INVESTIGATION ON NANOCOMPOSITES BEHAVIOUR UNDER BALLISTIC IMPACT

Antonio F. Ávila*, Marcilio Alves•, Ricardo L. Azevedo•
***Universidade Federal de Minas Gerais, Department of Mechanical Engineering**
6627 Antonio Carlos Avenue, Belo Horizonte MG 31270-901 Brazil
•Universidade de São Paulo, Department of Mechatronic Engineering and Mechanical Systems, 2231 Prof. Mello Morais Avenue, São Paulo SP 05508-900 Brazil

Abstract

This paper focuses on ballistic tests of a new class of composite materials, i.e. nanocomposites. The two nanoComposites studied are fiber glass/epoxy/nanoclay and fiber glass/epoxy/graphite nanoflakes. The fiber glass used is a plain weave 200 g/m^2, while the nanoclay is organically modified montmorillonite ceramic (Nanomer I30E) and the expandable graphite used to generated the nanoflakes was from Graftech (grade 160-80N).

Ballistic tests were performed considering two types of ammunition, i.e. 38 caliber and 9 mm full metal jacketed. The results showed that for a 38 revolver projectile a 5 mm thick nanocomposite was able to absorb the energy efficiently. A 9 mm projectile, with speed close to 380 m/s was stopped by a two plate (5 mm each) arrangement with elastic deformation of the second plate less than 18 mm. The energies during the ballistic tests ranged from 315 to 576 joules.

1 Introduction

Ballistic materials have been studied for years especially for military applications. However, after the 911 and Madrid terrorist attacks the usage of such materials become a valuable commodity for the ordinary citizen. Another aspect is the great increase of bullet proof vehicles in large cities such as São Paulo and Mexico City due to the increase on urban violence. Another issue was recalled by Caprino et al. [1] was the Concorde tragedy occurred in Paris in 2000, probably caused by a tire fragment moving at high speed and impinging the jet's fuel tanks, highlighted the importance of the impact behavior of aeronautical materials. Langdon et al. [2] also mentioned that a fiber-metal laminate luggage container was capable of withstanding a bomb blast greater than that in the Lockerbie air disaster.

As mentioned before a critical issue on ballistic materials, in addition to the impact resistance is weight. Composite materials are a valuable alternative to conventional materials due to their high specific mechanical properties, i.e. stiffness-to-weight and strength-to-weight, tailor-ability and damage tolerance. These composite materials and/or structures during their service life undergo various loading conditions. Among them, the most critical condition is the impact loadings due to the laminated nature of these structures. As stated by Luo et al. [3], the damage in composite structures resulting from impact events is one of the most important aspects to be considered in the design and applications of composite materials. Impact events, however, can be classified according to the impact velocity, i.e. low and high velocities. As mentioned by Naik and Shrirao [4], in high velocity impact, the contact period of the impactor is much smaller than the time period of the lowest vibration mode of the structure. As a consequence, the response of the structural element is governed by the local behavior of the material in the neighborhood of the impacted zone, the impact response of the element being generally independent of its support conditions.

According to Mines et al. [5], for high velocity impact, the perforation mechanics depend on the fiber type and volume fraction, the matrix, the stacking sequence, the size and initial kinetic energy of the impactor. Moreover, Cheng et al. [6] had demonstrated that penetration process can be broken down into three sequential stages: (i) punching; (ii) fiber breaking; and (iii) delamination. They even tried to model the perforation phenomenon by considering a failure criteria based into these three stages. Although their model presented good correlations against experimental results, they were limited to a 2-D axi-symmetric geometry. Gu [7] when further by adding the composite strain energy to his model. He was able to estimate the progressive damage and delamination caused by the high velocity impact. Potti and Sun [8], however, considered the use of the dynamic response model along with the critical deflection criterion to analyze the high velocity impact and perforation. They concluded that the delaminated area increases with the velocity up to the penetration ballistic limit. However, beyond this limit, the delamination area decreases with the increase of velocity. Abrate [9] mentioned that compressive strains in high velocity impact situations are inversely proportional to the stress wave propagation through the composite thickness. Still, in a small area near the impactor, this stress wave reaches the speed of sound, which supports the results presented by Potti and Sun [8].

In all cases, the key issue in the design of composite structures is the damage tolerance of each component, i.e. fibers and matrix. According to Silva Junior et al. [10], the use of aramid reinforced composites presents one of the best protections to weight ratio for impact applications. However, the high cost of these fibers is a disadvantage. One viable substitute to aramid fibers is the use of carbon fibers. Nevertheless, as mentioned by Davies and Zhang [11], carbon fibers epoxy composites have an elastic behavior but they are also brittle. So, they suggested the use of fiber glass reinforcement as carbon fiber replacement. Yet, fiber glass composite toughness is highly dependent on strain rate damage and the matrix behavior itself. A possible solution for this problem is to enhance the matrix toughness.

Findik and Tarim [12] suggested the usage of aluminum substrate and composite materials as another option to steel products. Following the same approach Villanueva and Cantwell [13] investigated the performance of fiber-metal laminates (FML) as skins of sandwich materials under high velocity impact conditions. They concluded that the application of aluminum foams associated to FML performed very well up to 120 joules. However, as stated by Findik and Tarim [12], the impact energy from fire arms ranges from low 700 joules from a 9 mm parabellum to high 2500 joules from a 7.62 caliber M1-rifle. Those values are far from the gas gun used by Villanueva and Cantwell.

An option to FML is the dispersion of nanoparticles into laminate composites, in special with epoxy systems. Yasmin et al. [14] were among those researchers who studied the effect of nanoparticles (organically modified montmorillonite - Cloisite 30B) into epoxy systems. By varying the amount of Cloisite 30B, in weight from 1% up to 10%, they observed an increase in the elastic moduli to a maximum of 80%. Another set of experiments on epoxy-nanoclay systems were conducted by Ho et al. [15]. They concluded both stiffness and toughness were enhanced by nanoparticles. However, for their binary system, resin - diglycidyl ether of bisphenol *A* and cure agent - triethylenetetramine, the ultimate tensile strength was obtained at 5% in weight of montmorillonite content. The difference between the Yasmin et al. [14] and the Ho et al. [15] results can be attributed to the mixing process, shear mixing in Yasmin's case and direct mixing for Ho's conditions. Consistent with Ho et al. [15], Avila et al. [16] not only reported an increase on ultimate strength for 5% content of montimonillonite, in their case Nanomer I30E from Nanocore Inc., but they also informed an increase on impact resistance close to 48%.

Kornmann et al. [17] studied the effect of another inorganic layered silicate in its nano-dimension form, i.e. fluorohectorite, into epoxy systems. According to them, like montmorillonite, the fluorohectorite has tremendous ability to exchange ions, which favors the penetration of the polymer or polymer precursors between these layers and consequently the formation of an exfoliated nanocomposite. They reported that with only 10 wt% of layered silicate added to the epoxy matrix, an increase of the Young modulus of 54% was noticed. However, the tensile strength was reduced by 36% and the elongation at break was also affected. When the nanomodified epoxy matrix was added to glass fibers, the results obtained by Kornmann et al. [17] were different. A remarkable increase in flexure strength, i.e. 27%, was observed while the Young's modulus enhanced only by 6%. Two hypotheses can explain this increase on flexural strength. First, the improvement on the compressive strength of the epoxy matrix is due to the presence of the layered silicate. The second is the presence of the silicate layers at the surface of the glass fibers, which may improve the interfacial properties between the matrix and the fibers.

So far, most of the scientific work has focused on the synthesis of polymer-layered silicate nanocomposites where a heating phase is present. This heating phase makes the nanocomposite manufacturing susceptible to premature degradation due to temperature gradients. The objective of this paper is to study the high velocity impact response of a polymer-nanoclay-fiber glass nano-structured laminate, where the heating phase is not present.

2 Experimental Procedures and Materials

The nanocomposites were manufactured following the procedure described in Avila et al. [16]. The ballistic tests were performed according to NIJ standard 0101.03 [18] for a type I and II-A classifications. Once the tests were performed the damaged areas were measured by image processing using the public domain software ImageJ 1.37 [19]. To characterize the effect of high strain rate behavior of nanocomposites specimens the split Hopkinson pressure bar was employed. Finally, the damaged plates were sectioned into beams and a three point bending tests were performed to evaluate the residual bending strength.

The fibers used during the nanocomposites preparation were plain weave fiber glass with 200 g/m^2 density. The epoxy formulation was based on *diglycidyl ether of bisphenol A* resin and a hardener, *triethylenetetramine*. The weight mixing ratio suggested by the manufacturer is 100A:20B, and the average viscosity is around 1257 cPs. The nanoclay employed was an organically modified montmorillonite in a platelet form, i.e. 10 μm long, 1 μm wide and 50 *n*m thick, called Nanomer I30E from Nanocor, while the graphite nanoflakes were from Graftech (grade 160-80N). The epoxy system/nanoparticles ratio studied were 0%, 5% and 10% with respect to the epoxy system weight. Moreover, the fiber/epoxy ratio was kept constant and equals to 65%.

3. Data Analysis

The high strain rate behavior was examined by the split Hopkinson pressure bar (SHPB) following the procedure suggested by Tsai and Huang [20]. As it can be observed in Figs. 1-3, the stress-strain curve has no significant difference between 0%, 5% and 10% nanoclay content for low strain rates.

When high strain rates are analyzed a trend can be identified. The dynamic stress-strain curves showed significant nonlinearity and strain-rate sensitivity. It seems that nanoclay content and its nanostructures formed, i.e. intercalated nanostructures, can also affect the composite viscoplastic behavior. Stiffness seems to be directly proportional to nanoclay content. An increase on strain rate leads to a correspondent increase on stiffness.

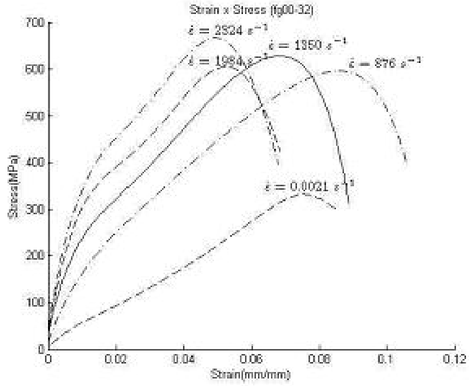

Fig. 1 Stress-strain curve for different strain rates – 0% nanoclay content

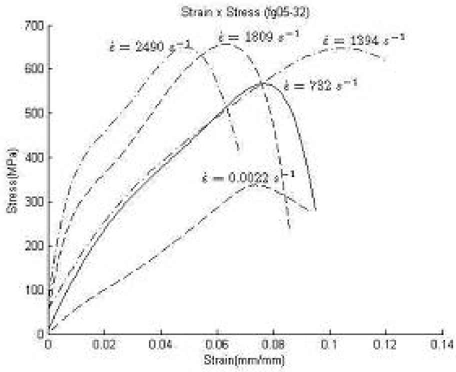

Fig. 2 Stress-strain curve for different strain rates – 5% nanoclay content

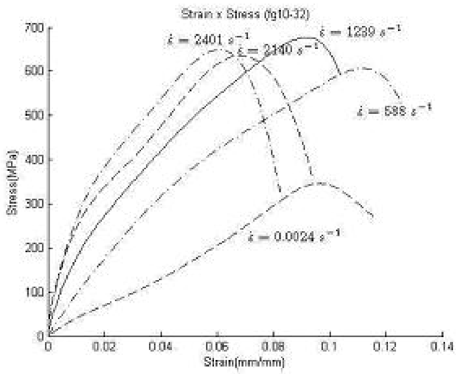

Fig. 3 Stress-strain curve for different strain rates – 10% nanoclay content

Furthermore, the highest stiffness was noticed for the 5% nanoclay content. Such observation can also corroborate the results presented by Avila and Silva Neto [21] where an unexpected decrease on stiffness for 10% nanocomposites was attributed to a precipitation of nanoclay clusters. Such hypothesis was supported by X-ray diffraction tests, where a reduction on X-ray diffraction intensity pointed out to an increase on system entropy. Such increase on entropy resulted into precipitation of nanoclay clusters, where the nanoclay original properties were retained. The white particles on micrographs showed in Fig 4 represent those nanoclay clusters.

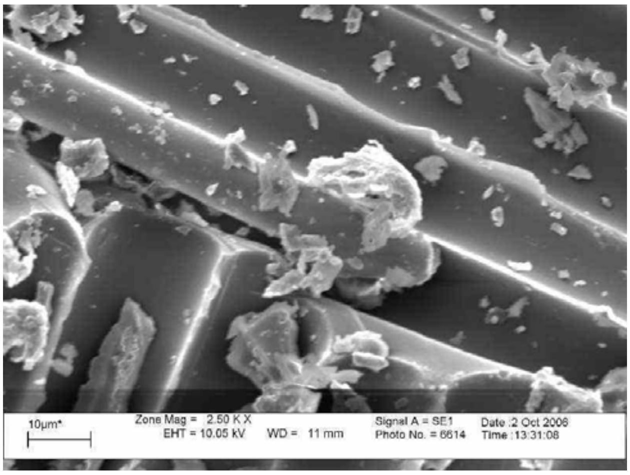

Fig. 4 SEM micrograph showing the nanocluster precipitation

The projectiles mass, impact velocity, energy transferred and type are listed in Table 1 and 2.

Table 1. Projectiles information

Test	Projectile Characteristics			
	Type	Mass [g]	Speed [m/s]	Energy [J]
1	9 mm FMJ	8.0	379.48	576.02
2	38 SLP	10.2	244.75	305.50
3	38 SLP	10.2	247.80	313.17
4	9 mm FMJ	8.0	379.48	576.02
5	38 SLP	10.2	246.28	309.34
6	9 mm FMJ	8.0	376.74	567.73
7	38 SLP	10.2	248.72	315.49
8	9 mm FMJ	8.0	373.08	556.76
9	9 mm FMJ	8.0	333.75	445.56
10	9 mm FMJ	8.0	332.54	442.33
11	9 mm FMJ	8.0	333.45	444.76
12	9 mm FMJ	8.0	335.28	449.65
13	38 SLP	10.2	234.09	279.47
14	38 SLP	10.2	244.14	303.98
15	38 SLP	10.2	243.23	301.72
16	38 SLP	10.2	235.92	283.86

A traditional way of analyzing damage influence on composites is the compression-after-impact test describe in ASTM standards [22]. However, in type of test, each plate is analyzed considering one centered damage region. For ballistic applications, where the number of impacted regions is much larger a different methodology has to be applied. Instead of evaluate the residual compression strength; the proposed methodology evaluated the residual bending strength. The residual bending properties are dependent on the damage extension and its location. Following Silva Jr et al. [10], the damage extension will be evaluated by the ration between the back and front damaged areas, a non-dimensional parameter defined as $\mu = BA/FA$. In addition to μ parameter another non-dimensional parameter (λ) is also defined as the ratio between the damaged area center of mass distance to the bending force application location and the distance between the location of the force application and the specimen semi-length. Notice that λ is defined in such way that when $\lambda \rightarrow 0$, the bending residual strength also leads to zero. Furthermore, when $\lambda \rightarrow 1$ the bending properties are approximately the ones from an undamaged specimen.

Table 2: Plates characteristics

Plate ID	Plate Characteristics
P2	Nanoclay 5%+ 1 ceramic layers of nanoclay 25%
P3	Nanoclay 5%+ 3 ceramic layers of nanoclay 25%
P4	Nanoclay 5%+ 1 ceramic layers of nanoclay 33%
P5	No nanoclay (pure fiber glass/epoxy)
P6	Nanoclay 5%
P9	No nanoclay (pure fiber glass/epoxy)
P10	Nanoclay 5%
P11	Graphite Nanoflake 3%

After the ballistic tests, the damage areas, i.e. back and front, were measured by image processing and from each plate and at least 6 bending specimens (50 mm wide x 350 mm long, and 5 mm thick) were prepared and tested. Figure 5A-5H show the load-deflection curves from each group tested. The bending strength was improved with the nanoclay and graphite nanoflakes dispersion into the epoxy matrix. Such observation is corroborated by the slopes of the load-deflection curves.

The residual bending stress, as observed before, is dependent of the location and its extension. Figure 5H, case 11-6, shows the smallest residual bending stiffness measured. This is due to the combination of extensive damage, which can be translated in a large μ (>1.5) and a small distance from the bending force application, i.e. λ <0.2. When the bending force is applied the stress distribution around the damage area becomes non-uniform with points where stresses easily reach beyond the elastic limit. A considerable increase on fiber breakage was introduced and the bending stiffness reduced.

When the residual bending strength was analyzed considering only the undamaged bending specimens, e.g. P2-1, P5-1 and P11-1, and increase of 32.69% and 30.77% was observed with the inclusion on nanoclay and nanoflakes, respectively.

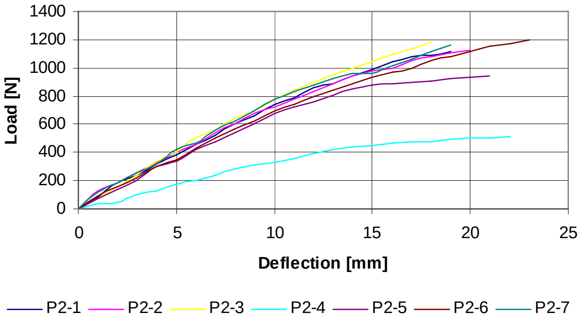

(a)

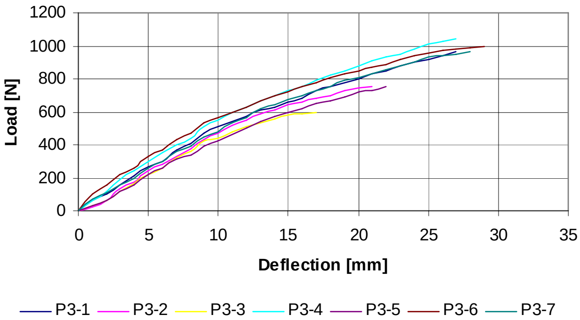

(b)

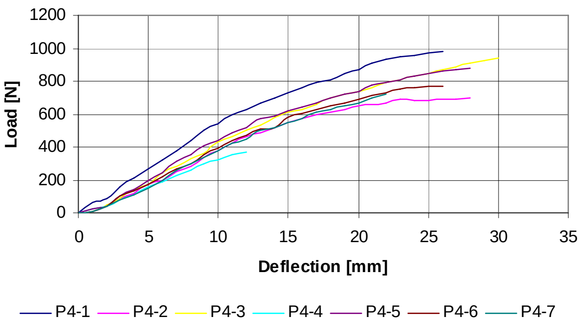

(c)

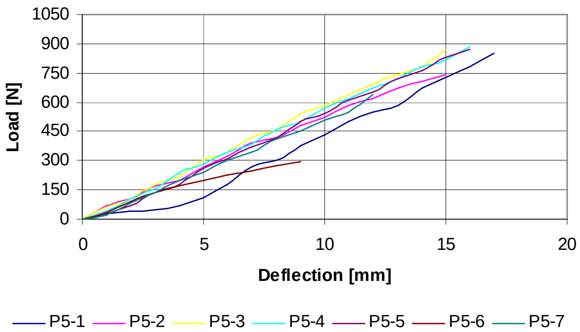

(d)

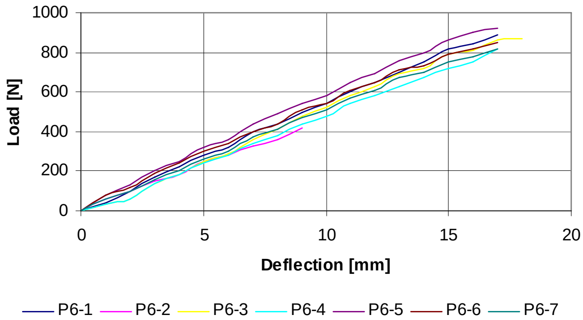

(e)

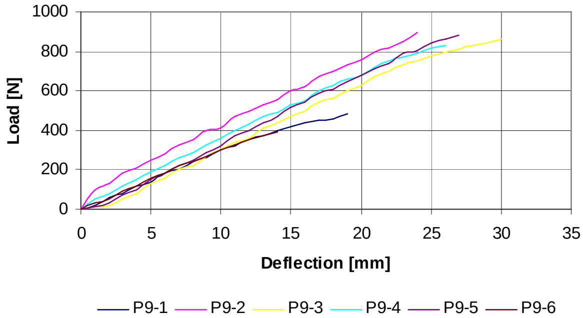

(f)

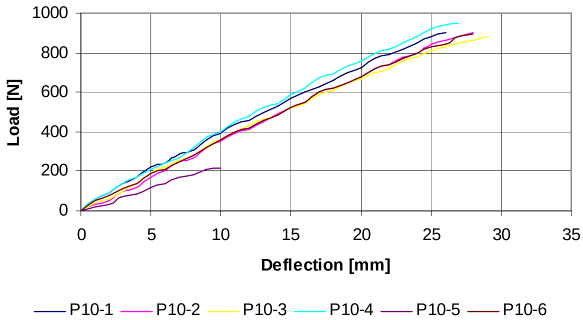

(g)

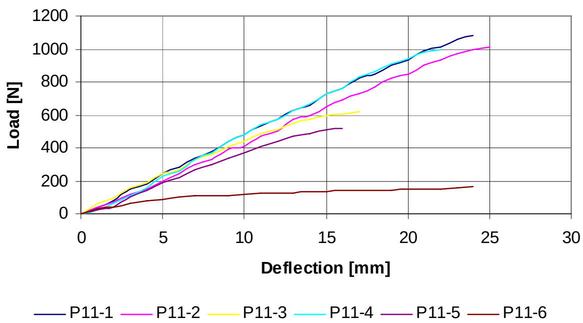

(h)

Fig. 5 Bending load-deflection plots. (a) plate P2, (b) plate P3, (c) plate P4, (d) plate P5, (e) plate P6, (f) plate P9, (g) plate P10, (h) plate P11.

Tables 3 and 4 summarize the data obtained after each fire test. Each damaged area was measured by image processing technique; at least 6 measurements were performed. The delaminated area, back (BA) and front (FA), and the back elastic deformation (BED) were measured. In most cases three distinct damaged areas were noticed on back area, while two different regions, i.e. projectile impact and delamination areas were observed. The occurrence of perforation was also detected.

Table 3: Ballistic test results

Test ID	Plate ID	BED [mm]	Perforation
1	P3	-----	YES
2	P3	5.0	NO
3	P2	7.5	NO
4	P2	-----	YES
5	P4	8.0	NO
6	P4	-----	YES
7	P5	13	NO
8	P5+P6	16	NO
9	P9+P10	13	YES
10	P9+P10	16.2*	YES
11	P9+P11	17.0*	YES
12	P9+P11	8.2	NO
13	P10	-----	YES
14	P10	7.9	NO
15	P11	14.0	NO
16	P11	11.5	NO

* Damaged cone measured

Table 4: Damaged areas, λ and μ variables

ID	BA[mm²]	FA[mm²]	μ	λ
1	2811.94±41.23	771.35±42.32	3.65±0.15	0.486
2	10899.12±43.79	1340.85±44.74	8.14±0.23	0.592
3	5586.71±29.63	501.38±20.14	11.16±0.39	0.514
4	3921.74±30.69	2652.18±43.33	1.48±0.01	0.383
5	4993.56±18.67	6866.08±16.72	0.73±0.01	0.457
6	5158.38±39.44	2893.93±11.59	1.78±0.06	0.314
7	3761.95±25.81	4345.73±66.51	0.87±0.01	0.240
8*	3103.29±38.64	550.02±38.53	5.67±0.33	0.286
	5295.82±38.09	4431.03±28.74	1.19±0.01	
9*	2962.22±58.58	231.29±3.93	12.84±0.03	0.142
	3286.00±47.76	2395.15±48.07	1.37±0.08	
10*	1388.82±16.25	231.29±3.93	6.01±0.03	0.371
	1849.23±77.19	1175.53±24.77	1.57±0.03	
11*	1032.23±10.08	231.30±3.93	4.46±0.03	0.429
	3086.22±31.12	1029.95±15.64	2.99±0.01	
12*	1215.46±17.04	231.32±3.92	5.26±0.02	0.657
	3090.33±15.73	1329.92±60.37	2.33±0.09	
13	2118.21±43.94	1681.25±61.11	1.26±0.02	0.771
14	3528.30±95.25	2394.23±46.71	1.47±0.01	0.800
15	2962.69±30.51	1825.87±24.79	1.62±0.01	0.171
16	2616.69±34.91	1518.31±42.98	1.72±0.03	0.714

* Plate position according to table 3

From Tables 3 and 4, it is possible to conclude that there is an increase on delamination with the presence of nanoparticles, i.e. nanoclay and graphite nanoflakes. According to Silva Jr. et al. [10], the delamination failure is the most common mechanism of energy absorption. In this investigation, the μ parameter reached the 12.84 mark, an indication of good performance. Furthermore, when the two plates are associated in series, i.e. cases 8-12, the results are very good. Yet, despite of the large vales of μ, in two cases the perforation was noticed. This phenomenon suggests that not only the delamination mechanism is present during the impact event.

The ballistic cone formation due to the projectile compression on target, mentioned by Naik and Shrirao [4], can be the cause another failure mechanism presence. When the ballistic cone is formed, in addition to the local compressive loading, a bending stress is also applied, mainly into the surrounding areas of the projectile impact. Tension and compression loading are developed through the composite thickness. Micro-buckling, due to the compression stresses developed during the bending can be the cause of failure into the fibers close to the internal region (front area). At same time, fiber breakage is occurring due to tension on the back area. Such mechanism also leads to delamination due to the shear stress generated between layers.

In their study, Naik and Shrirao [4], did not considered the projectile deformation as a source of damage inside the composite. Figure 6 shows the case where the 38 caliber projectile after penetration of some layers "spread" between layers. In this case, the μ parameter, indicates a low performance, as its value is low. However, due to the nature of the damage, the μ parameter is not enough to evaluate the ballistic performance. The back elastic deformation and the perforation condition must be considered. Furthermore, by analyzing the BED (≈ 13 mm) and perforation condition, according to the NIJ standard [18], the composite performance is acceptable.

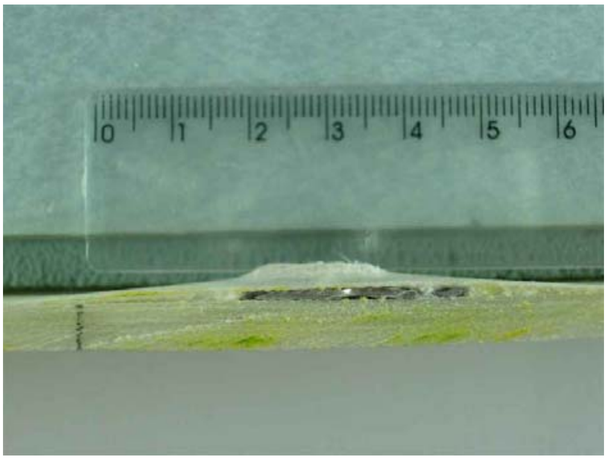

Fig 6. 38 caliber impact in a fiber glass/epoxy

A different behavior has noticed when the amount of nanoclay was increased on the front area, e.g. case P4. During the 38 caliber impact on a P4 nancomposite the projectile hits the plate and rebounds. Such fact can be attributed to the nanoclay layer. However, this rebound also caused an extensive damage as shown in Fig. 7.

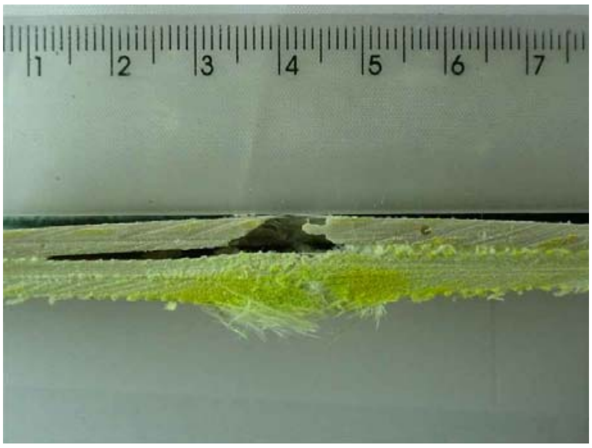

Fig. 7. 38 caliber impact in a P4 nanocomposite

The 9 mm FMJ impact also was affected by the nanoclay/graphite nanoflakes presence. Figures 8-9 show the failure mechanism in these cases. The extra nanoclay layer disbanded from the fiber glass/epoxy/nanoclay part when the number of layers increased from 1 (P2 condition) to 3 (P3 condition), or the amount of nanoclay increased from 25% (P2) to 33% (P4). Such fact can be attributed to the local increase on stiffness, which creates “a shield” for the laminate.

Fig. 8. 38 caliber impact in a P3 nanocomposite

The addition of nanoclay and graphite nanoflakes has direct influence on high velocity impact resistance of laminate composites. However, the failure mechanisms and damage generated is also dependent of the amount of such nanoparticles disperse, how they are dispersed and the ammunition used during the ballistic tests. Due to the nature of graphite nanoflakes, another hypothesis can also be formulated. The presence of nanoparticles increases the friction coefficient between projectile and target, inducing an addition deformation to the bullet and increasing the energy absorption. Figure 10 shows a transverse cut of a P11 plate. Notice that in this case the 9 mm projectile was trapped inside the damage area.

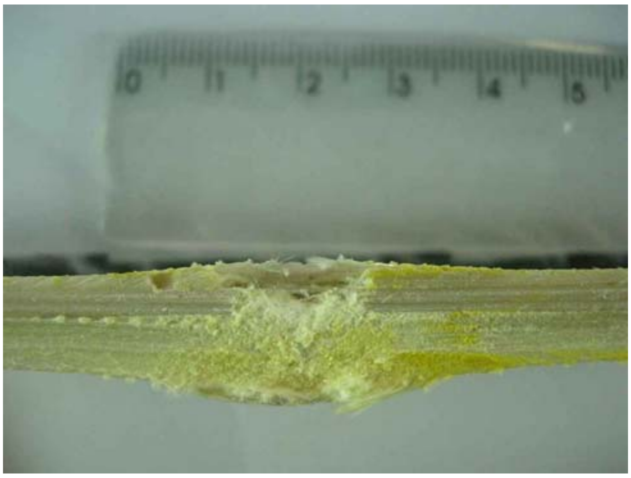

Fig.9 9 mm FMJ impact in a P2 nanocomposite

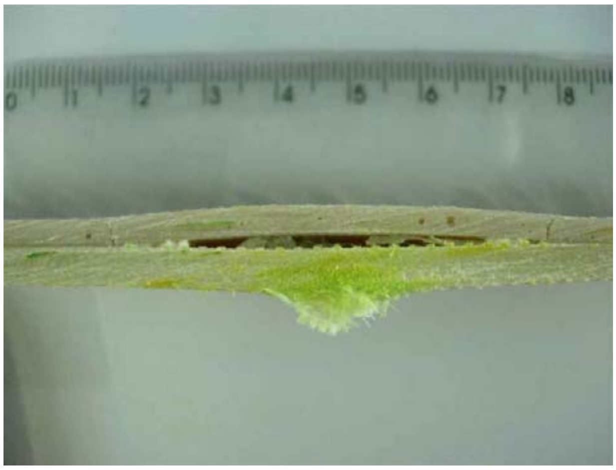

Fig.10 9 mm FMJ impact in a P4 nanocomposite

The different failure mechanisms are consequence of the type of target tested and the ammunition used, as shown in Figure 11. However, the usage of nanoparticles, nanoclays or graphite nanoflakes, seems to be a valuable addition to the composite. Notice that nanoparticles/nanoflakes have direct effect on composite strain rates, as demonstrated by the SHPB tests. Moreover, the bending strength is also affected by the nanoparticles addition to the composite.

Fig. 10 9 mm trapped inside the damage area

Fig. 11. Bullets after impact

4. Conclusion

The addition to nanoclay and graphite nanoflakes to fiber glass/epoxy laminates not only increases the high velocity impact resistance of such composites, but it also has influence of failure mechanism. Following the NIJ standard, it is possible to classify the nanocomposites studied can as an armor type I for a 5 mm thickness and a type II-A when the thickness is equal to at least 10 mm.

Acknowledgement

The authors would like to acknowledge the Brazilian Research Council (CNPq) grant 471585/2004-1, the São Paulo State Research Foundation (FAPESP) grant 04/15405-7 for their financial support. We also would like to recognize Dr. Cláudia A. Vanetti and the Center of Microscopy and Microanalysis of Universidade Federal de Viçosa (NMM/UFV/FINEP) for usage of the SEM. Finally, we would like to express our gratitude to all personnel involved during the ballistic tests, in special to lieutenant Leonardo Castro from the Minas Gerais State Police Department and Mr. Alisson Duarte from the Mechanical Engineering Department.

References

[1] Caprino G., Lopresto V., Santoro D. “Ballistic impact behavior of stitched graphite/epoxy laminates.” *Composites Science and Technology*, Vol. 67, No. 2, pp 325-335, 2007.

[2] Langdon G.S., Lemarski S.L, Nurick G.N., Simmons M.C., Cantwell W.J., Scheleyer G.K. “Behavior of fibre-metal laminates subjected to localized blast loading: Part I – Experimental observations.” *International Journal of Impact Engineering*, Vol. 34, No. 8, pp. 1202-1222, 2007.

[3] Luo R.K., Green E.R., Morrison C.J. “Impact damage analysis of composite plates.” *International Journal of Impact Engineering*, Vol. 22, No. 5, pp 435-447, 1999.

[4] Naik N.K., Shrirao P. “Composite structures under ballistic impact.” *Composite Structures*, Vol. 66, No. 8, pp 578-590, 2004.

[5] Mines R.A.W., Roach A.M., Jones N. “High velocity perforation behavior of polymer composite laminates.” *International Journal of Impact Engineering*, Vol. 22, No. 6, pp 561-588, 1999.

[6] Cheng W.L., Langlie S., Itoh S. “High velocity impact of thick composites.” *International Journal of Impact Engineering*, Vol. 29, No. 2, pp 167-184, 2003.

[7] Gu B. “Analytical modeling for ballistic perforation of planar plain-woven fabric target by projectile.” *Composites Part B*, Vol. 34, No. 3, pp 361-371, 2003.

[8] Potti S.V., Sun C.T. “Prediction of impact induced penetration and delamination in thick composite laminates.” *International Journal of Impact Engineering*, Vol.19, No. 1, pp 31-48, 1997.

[9] Abrate S. “*Impact on Composite Structures*.“ 1st edition, Cambridge:Cambridge UP, 1998.

[10] Silva Junior J.E.L., Paciornik S., d’Almeida J.R.M. “Evaluation of effect of ballistic damaged area on the residual impact strength and tensile stiffness of glass-fabric composite materials.” *Composite Structures*, Vol. 64, No. 1, pp 123-127, 2004.

[11] Davies G.A.O., Zhang X. “Impact damage prediction in carbon composite structures.’ *International Journal of Impact Engineering*, Vol.16, No. 1, pp 149-170, 1995.

[12] Findik F., Tarim N. “Ballistic impact efficiency of polymer composites.” *Composite Structures*, Vol. 61, No. 1, pp 187-192, 2003.

[13] Villanueva G.R., Cantwell W.J. “The high velocity impact response of composite and FML-reinforced

sandwich structures.", *Composites Science and Technology,* Vol. 64, No. 1, pp 35-54, 2004.

[14] Yasmin A., Luo J-J., Daniel I.M. "Processing of graphite nanosheet reinforced polymer nanocomposites." *Proceedings of the 19th ASC/ASTM Joint Technical Conference*, Atlanta (Georgia, USA),Vol.19, CDROM, 2004.

[15] Ho M-W., Lam C-K., Kau K-T., Ng D.H.L., Hui D. "Mechanical properties of epoxy-based composites using nanoclays." *Composites Structures*, Vol. 75, No. 3, pp 415-421, 2006.

[16] Avila A.F., Soares M.I., Silva Neto A. "A study on nanocomposites laminated plates behavior under low velocity impact." *International Journal of Impact Engineering*, Vol. 34, No. 1, 28-41, 2007.

[17] Kornmann X., Rees M., Thomann Y., Necola A., Barbezat M., Thomann R. "Epoxy-layered silicate nanocomposites as matrix in glass fiber-reinforced composites." *Composites Science and Technology,* Vol. 65, No. 10, pp 2259–2268, 2005.

[18] NIJ Standard 0101.03 "Ballistic resistance of police body armor." U.S. Department of Justice, National Institute of Justice, Washington DC, pp 1-13, 1987.

[19] Rasband W. ImageJ 2006.URL: http://rsb.info.nih.gov/ij/

[20] Tsai J-L., Huang J-C. "Strain rate effect on mechanical behaviors of nylon 6-clay nanocomposites." *Journal of Composite Materials*, Vol. 40, No. 10, pp. 925-938, 2004.

[21] Ávila A.F, Silva Neto A. "The influence of intercalated nanoclay into nanocomposites impact behavior." *Proceedings of the 2006 ASME International Mechanical Engineering Congress and Exposition*, Chicago, DVD, 2006.

[22] ASTM standard D 7137/7137M "Standard Test Method for Compressive Residual Strength Properties of Damaged Polymer Matrix Composite Plates", *Annual ASTM Book*, Vol. 08, No. 01, pp. 450-463, 2005.